Semiclassical Monte Carlo with quantum-confinement enhanced scattering

Quantum correction and application to short-channel device performance vs. mobility for biaxial-tensile-strained silicon nMOSFETs

Ningyu Shi, Leonard F. Register and Sanjay K. Banerjee

Dept. of ECE and Microelectronics Research Center, The University of Texas at Austin

Austin, TX, USA

Email: ningyushi@mail.utexas.edu

Abstract—**A model of valley-dependent quantum-confinement-enhanced scattering has been added to existing quantum corrections in our full band Monte Carlo simulator, *Monte Carlo of the University of Texas* (MCUT) [1]. The simulator was then calibrated to fit mobility curves, both strained and unstrained, by adjusting surface roughness parameters. By comparing mobility and device simulation results, we find significant deviations in short channel strained Si nMOSFET performance — some potentially beneficial — from expectations based on mobility and thermal velocity alone.**

Keywords - Full-Band Monte Carlo; Strained Si; Quantum correction; Mobility.

I. INTRODUCTION

Strain is widely used to increase the potential performance of devices independent of geometric scaling [2]. Strain alters the bandstructure of conduction and valence band(s). For example, by applying biaxial tensile strain to bulk silicon (Si), energy valleys with lower conductivity effective masses in the direction of transport can be lowered in energy relative to those with higher conductivity effective mass, so that the former are occupied, intervalley scattering is reduced, and, thus, mobility is increased.

However, improvements in bulk mobility do not necessarily translate to proportional changes in channel mobility, not only because of surface roughness but also due to quantum confinement effects including but not limited to degeneracy breaking among energy valleys, e.g. [3,4]. And changes in channel mobility do not necessarily translate to proportional changes in drive current in short channel MOSFETs where non-local field effects are the norm, and ultimate device performance is limited by thermal velocities. And, although scattering remains critical to understanding the performance of short-channel devices, scattering processes in short channel devices do not add in the same way they do in mobility calculations, as exhibited in, e.g., [5]. Predictive transport simulations for short channel devices require all of these effects to be considered simultaneously.

To address the challenge of both strain and quantum confinement effects for short channel devices in this work, our full-band semiclassical Monte Carlo device simulator, Monte Carlo of The University of Texas (MCUT) is used with valley-dependent quantum corrections [1], including recently added ones for quantum-confinement enhanced scattering.

II. VALLEY-DEPENDENT QUANTUM-CONFINEMENT-ENHANCED SCATTERING

A. Basic Theory

In the inversion layer of n-channel Si MOSFETs, the degeneracy among the six Δ valleys will be broken via confinement-induced and effective-mass dependent sub-band energy shifts. Thus, quantum confinement will not only redistribute the carriers in real space away from the oxide-channel interface, but also among energy valleys toward the lower energy valleys. And with increasing valley-edge splitting, f-type intervalley scattering becomes increasingly unlikely as carriers are increasingly localized to the lower minimum energy valleys. The changes affect capacitance, conductivity effective masses, and momentum and energy relaxations rates. MCUT uses valley-dependent quantum corrections to address each of these issues, corrections which shift the (now quantum-corrected) valley edges to match the classical charge carrier distributions to the quantum mechanical ones — obtained via self-consistent solution of the Schrödinger and Poisson equations — as a function of position along and normal to the plane of the channel, and among energy valleys (actually quadrants of the Brillouin zone), much as has been described in detail previously [1].

However, quantum confinement can also affect intra-valley and g-type inter-valley scattering rates, ultimately increasing scattering rates for strong confinement, e.g. [3,4]. To address this latter issue, a quantum correction for modeling quantum-confinement-enhanced scattering scheme has been introduced in (MCUT). As illustrated by Figure 1 for inter-valley phonon scattering of energy $\hbar\omega$ in the absence of strain, the pre-calculated and potentially strain-dependent scattering rates are looked up, based on the quantum-corrected (qc) *total* energy of the final (*f*) states, that referenced to the uncorrected valley edge energies, $E_{f,total} = E_f(\mathbf{k}_f) + \Delta E_{qc}(valley_f)$. In other words, as the free carrier motion follows the quantum-corrected potentials, the carrier scattering rates follow the uncorrected

potentials. As increasing confinement drives the quantum corrections up for, in particular, the final states, it drives the scattering rates up as well. If $E_f(\mathbf{k}_f)$ is less than zero, however, the scattering process is nevertheless disallowed even when the pre-calculated scattering rate as a function of $E_{f,total}$ is nonzero.

$$E_{i,total} = E_i(\mathbf{k}_i) + \Delta E_{qc}(valley_i)$$
$$E_{f,total} = E_f(\mathbf{k}_f) + \Delta E_{qc}(valley_f)$$
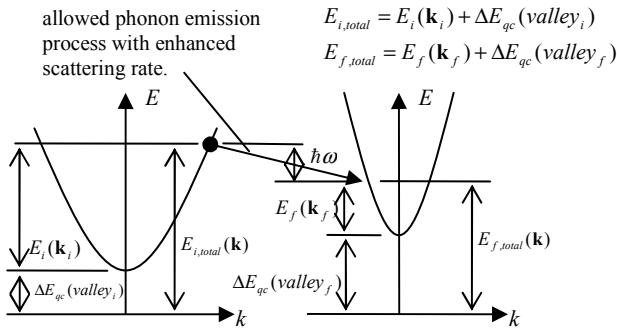
Figure 1. Modeling of quantum confinement-enhanced scattering. Scattering rates are based on total energy $E_{f,total}$ including the quantum correction.

B.   *Effects of valley-dependent quantum confinement, etc.*

To test the effects of the valley-dependent quantum-confined scattering, we ran the simulator for unstrained and biaxially-strained 50 nm channel length n-channel MOSFETs, with and without valley-dependent quantum corrections. The parameter set listed in Table 1 was used. All other parameter including surface roughness to be discussed below, were held constant in these simulations. In the Cases A, B and C, the strain-induced valley splitting of 168 meV between the Δ_2 and Δ_4 valleys is enough to reduce the relative occupation of the latter valleys by over a factor of 600 at the 300K simulation temperature for a near-equilibrium carrier distribution, at least for a Boltzmann distribution (although we note that Pauli-exclusion is modeled in the simulations). Only in Cases A (with strain) and D (without strain) are valley-dependent quantum corrections used. In Cases C (with strain) and E (without strain) the density of states effective mass per valley, 0.328 m_e, was used to calculate the quantum corrections for all valleys. In Case B (with strain) the quantum corrections for all valleys were calculated based on that appropriate for the Δ_2 valleys only.

Comparison of Cases A and C and of Cases D and E demonstrate that using one average effective mass to obtain the quantum corrections can lead to underestimation of the drive current. In Cases A and C (and B) with the large valley splitting scattering, f-type intervalley scattering would be greatly reduced, independent of the quantum correction model. Therefore the principal reasons for the differences in current are likely differences in calculated real-space carrier distributions and quantum confinement-enhanced intravalley and g-type intervalley scattering resulting from using different effective masses for the quantum corrections in Case A. In Cases D and E with no strain, the *relatively* greater difference in the currents may well be traceable to both the quantum-confinement-induced segregation of carriers to the Δ_2 valleys and reduced f-type intervalley scattering in Case D, neither of which can be addressed with valley-independent quantum corrections.

Beyond the issue of quantum corrections *per se*, comparison of Cases A and B point to the continuing importance of hot carriers and self-consistent electrostatics in short-channel MOSFETs, considerations unimportant to low-field mobility or thermal velocity. With the large strain-induced valley splitting and the same mass used for calculation of the quantum corrections in the low-energy Δ_2 valleys, differences between Cases A and B can only be associated with — presumably down-channel — hot carriers which can access the higher lying Δ_4 valleys. Furthermore, the increasing difference in currents at higher gate voltages when there are more carriers in the channel, suggests that the difference is due more to electrostatically self-consistent changes to reduce the electric field *along*-channel near the barrier top, rather than due to direct backscattering. In these simulations, this change is likely associated with the relative slowing down of some hot carriers via scattering to the Δ_4 valleys which are more accessible in Case B. The difference in these currents, however, only reflects the difference in self-consistent electrostatic effects, for the fraction of hot carriers scattering to the Δ_4 valleys, due to the difference in the mass-dependent quantum corrections, on the field along the channel. The total effect of scattering and even just hot carrier scattering on the potential profile along the channel can be expected to be significantly larger.

Table I: Simulation parameters

Case	Strain	Δ_2 valleys		Δ_4 valleys	
		Confinement effective mass (m_e)	Strain-induced valley-edge shift only (eV)	Effective mass (m_e)	Strain-induced valley-edge shift only (eV)
A	Y	0.19	0	0.98	0.168
B	Y	0.98	0	0.98	0.168
C	Y	0.328	0	0.328	0.168
D	N	0.19	0	0.98	0
E	N	0.328	0	0.328	0

Note that the lowest energy valley minimum is used as the zero energy reference, and all simulations employ one set, the unstrained set, of SR parameters.
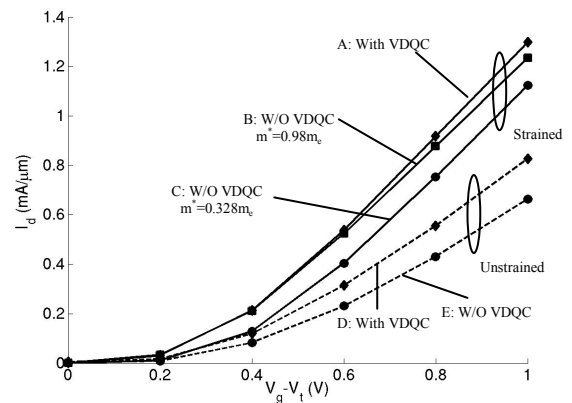
Figure 2. Current comparison with and without valley-dependent quantum corrections (VDQCs) for 50 nm channel length unstrained and biaxially strained n-channel MOSFETs.

III. Mobility calibration of strained Si

The simulator was first calibrated to strained bulk mobility via adjustment of the relative strengths of g-type and f-type phonon scattering deformation potentials. After the initial tests of Section II, the surface roughness (SR) parameters were then set via comparison of simulated mobility to measure channel mobilities for strained Si [6]. We note however, that the confinement-enhanced scattering, which alone reduces the channel mobility by perhaps a factor of two or more, also therefore significantly reduces the extracted surface roughness from what would be obtained otherwise. Furthermore, as was previously found via comparison of mobility to fully quantum mechanical (vs. quantum corrected) calculations of quantum-confined channel mobility [4] and in first-principles calculations of "surface roughness" [7], we also found that it's not possible to fit both strained and unstrained experimental mobility curves by using one set of SR parameters, as shown in Figure 3. Instead we reduced SR scattering in the strained case by varying the magnitude of the rms surface roughness displacement amplitude Δ_{SR} while keeping the correlation length of the surface roughness the same. E.g., for $Si_{0.75}Ge_{0.25}$, the Δ_{SR} the extracted strained SR scattering is 40% of the unstrained case, similar to the approximately 50% value that was obtained via more rigorous quantum mechanical mobility calculations of [4].
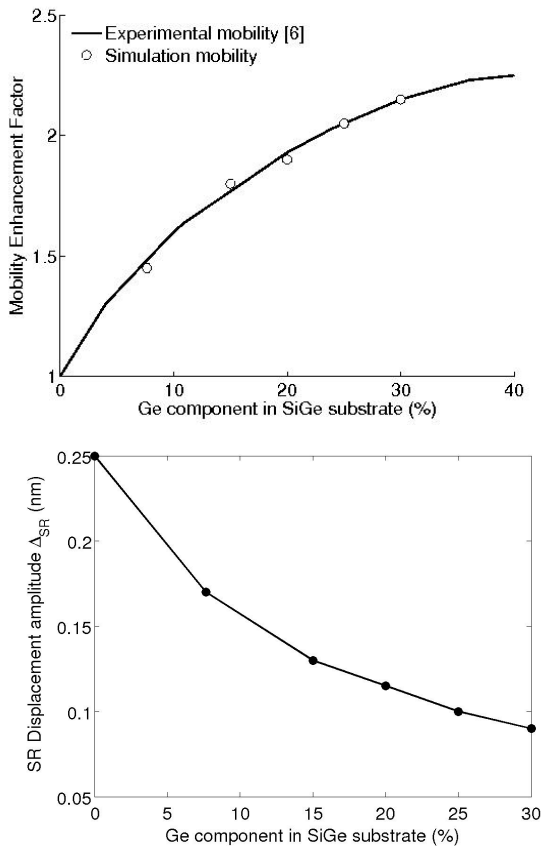
Figure 3. (top) Experimental and simulated mobility in Si MOSFET channels as a function of Ge mole fraction in the SiGe substrate, and (bottom) the corresponding SR displacement amplitudes vs. Ge mole fraction required to match experimental and simulated mobility.

IV. Mobility and device simulation result compared

Figure 4 shows that bandstructure-related effects of biaxial strain — surface roughness amplitude was again held constant at its unstrained value for this simulation — can be larger for drive current in, here, a 50 nm channel length device [8] than for mobility, despite approaching the ballistic limit, and can continue to increase with increasing strain after mobility benefits saturate. The limited and quickly saturating effect on low-field mobility results from strong quantum confinement that largely pre-segregates cool carriers to the low conductivity effective mass Δ_2 valleys. For high-field mobility, mobility is more greatly affected because hot carriers are still influenced by the increasing intervalley energy gap, but still not as significantly as for the drive current. The greater effects on the device current are likely due to reduced down-channel hot-carrier scattering and an associated self-consistent reduction in the field near the barrier top to reduce backscattering of subsequent electrons, much like in Section II the for Cases A and B of Table I and Figure 2.

Figure 5 shows the additional effect of varied surface roughness parameters that are, in contrast, much more significant for mobility than for short-channel MOSFET performance. We note that, e.g., while phonon scattering can cause backscattering in MOSFETs, optical phonon emission that does not cause backscattering, can actually reduce elastic backscattering by lowering the carrier energy. Thus, reduced effects of surface roughness scattering and non-Mathiessen's rule like behaviors should not be unexpected in short channel devices, and has been exhibited previously in, e.g., the fully quantum transport simulations of [5] along with scattering-related self-consistent changes in field along the channel. In the end, the net drive current improvement here is about one-half that of the mobility improvement, as one might expect for being about half way to the ballistic limit based on more simple theory and mobility changes [9]. However, the path to this drive current change is, in fact, quite different.
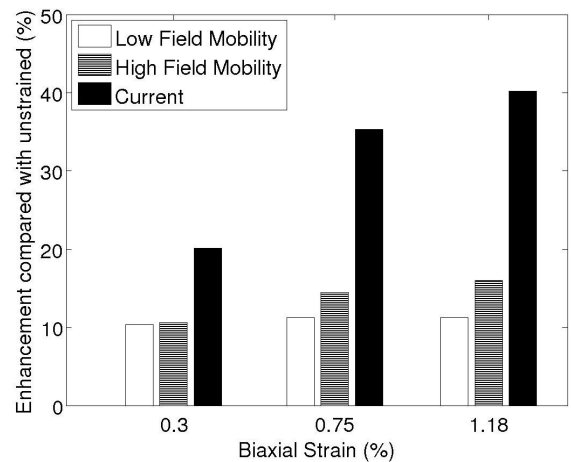
Figure 4. Strain effects on device drive current, low field mobility, and high field mobility for a 50 nm channel length well-tempered MOSFET [8], for an ~1MV/cm effective confinement field and fixed (unstrained) surface roughness.
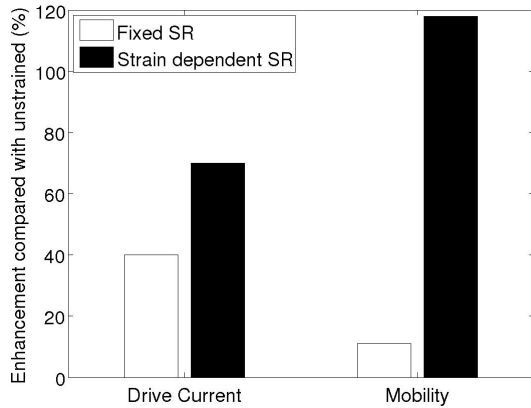
Figure 5. Strain effects on device drive current and low-field mobility for an ~1MV/cm effective confinement field with fixed and with strain-dependent surface roughness.

V. CONCLUSION

A model of valley-dependent quantum-confinement-enhanced scattering has been implemented, along with prior valley-dependent quantum corrections for redistribution of carriers in real space and among energy valleys, in the semiclassical Monte Carlo device simulator MCUT. With this simulator we find a strain-dependence in the surface roughness via comparison to experimental mobility calculations, consistent with prior fully quantum mechanical calculations of mobility [4]. Furthermore, while it is these differences in surface roughness that appear to be predominantly responsible for strain-induced changes in mobility, again consistent with [4], we find that changes in the bandstructure are more important to short-channel MOSFET performance. Beyond the consideration of strain, the observed relatively smaller effect of surface roughness changes on drive current as compared to mobility may have positive implications for use of high-k gate stacks and or in other material systems where increases in surface roughness are a concern. More generally, in this work, we have demonstrated that cumulative scattering that does not obey Mathiessen's rule, hot carriers, and *self-consistent* changes in the electric field along the channel remain important to determining short channel MOSFET performance, not just thermal velocity and low-field mobility. In a related work [10], we have used these quantum corrections to explore alternate surface and channel orientation, uniaxial strain, and scaling from 50 to 13 nm channel lengths.

REFERENCES

[1] X. Fan, et. al., "MC simulation of strained-Si MOSFET with full-band structure and quantum correction", *IEEE Trans. Electron Devices*, vol. 51, pp. 962-970, 2004

[2] Minjoo L. Lee and Eugene A. Fitzgerald, Mayank T. Bulsara, Matthew T. Currie, and Anthony Lochtefeld, "Strained Si, SiGe, and Ge channels for high-mobility metal-oxide-semiconductor field-effect transistors", *J. Appl. Phys.* vol. 97, pp. 011101, 2005

[3] Shinya Yamakawa, et al, "Study of interface roughness dependence of electron mobility in Si inversion layers using the Monte Carlo method" *J. Appl. Phys.* vol. 79, pp. 911-916, 1996.

[4] M. V. Fischetti, et al., "On the enhanced electron mobility in strained-silicon inversion layers", *J. Appl. Phys.* vol. 92, pp. 7320-7324, 2002.

[5] K.-M. Liu, W. Chen, L. F. Register and S. K. Banejee, "Schrödinger equation Monte Carlo-3D for simulation of Carrier transport in Nanowired MOSFETs," *J. App. Phys.* 104, 114515 (Dec, 2008).

[6] K. Rim, et al., "Fabrication and Mobility Characteristics of Ultra-thin Strained Si Directly on Insulator (SSDOI) MOSFETs", *IEEE IEDM*, pp 49-52, 2003

[7] G. Hadjisavvas, et al., "The Origin of Electron Mobility Enhancement in Strained MOSFETs,", *Electron Device Lett.*, vol. 28, pp. 1018-1020, 2007

[8] MIT well-tempered MOSFETs:
http://www-mtl.mit.edu/researchgroups/Well/

[9] Lundstrom, M. "Elementary scattering theory of the Si MOSFET", *Electron Device Lett.*, vol. 18, pp. 361-363, 1997

[10] N. Shi, L. F. Register and S. K. Banerjee, "On strain and scattering in deeply-scaled n-channel MOSFETs: a quantum-corrected semiclassical Monte Carlo analysis", *IEEE IEDM*, 2008